The Cryosphere Discuss., doi:10.5194/tc-2016-84, 2016
Manuscript under review for journal The Cryosphere
Published: 18 April 2016

The Cryosphere Discussions
Open Access
EGU

Temporal evolution of weak layer and slab properties in view of snow instability

Jürg Schweizer, Benjamin Reuter, Alec van Herwijnen, Bettina Richter, Johan Gaume

WSL Institute for Snow and Avalanche Research SLF, Flüelastrasse 11, 7260 Davos Dorf, Switzerland

Correspondence to: Jürg Schweizer (schweizer@slf.ch)

Abstract. If a weak snow layer below a cohesive slab is present in the snow cover, unstable snow conditions can prevail for days or even weeks. We monitored the temporal evolution of a weak layer of faceted crystals as well as the overlaying slab layers at the location of an automatic weather station in the Steintälli field site above Davos (Eastern Swiss Alps). We focussed on the crack propagation propensity and performed propagation saw tests on seven sampling days during a two-month period from early January to early March 2015. Based on video images taken during the tests we determined the mechanical properties of the slab and the weak layer and compared them to the results derived from concurrently performed measurements of penetration resistance using the snow micro-penetrometer (SMP). The critical cut length, observed in PSTs, showed a distinct pattern of temporal evolution that differed from the trend of other mechanical properties suggesting that it is not possible to assess crack propagation propensity by simply monitoring some of the relevant mechanical properties. A simple sensitivity study showed the complex interplay between these properties. Traditional and newly-developed metrics of snow instability describing either the failure initiation or the crack propagation propensity, calculated from simulated snow stratigraphy (SNOWPACK) or derived from the SMP signal, did partially reproduce the observed temporal pattern. Whereas our unique dataset of quantitative measures of snow instability provides new insights into the complex slab-weak layer interaction, it also showed some deficiencies of the modelled metrics of instability – calling for an improved representation of the mechanical properties.

1 Introduction

Dry-snow slab avalanche release is governed by failure processes within the layered snowpack. Whether a failure initiates and a resulting macroscopic crack eventually propagates, depends on the complex interaction between slab layers, the weak layer and to some extent the base layers, i.e. the layers below the weak layer. For example, considering the slab, the thickness and characteristics of the slab layers determine how much stress due to a skier is transferred to the depth of the weak layer (Habermann et al., 2008; Monti et al., 2016; Thumlert and Jamieson, 2014), but also how much deformation energy can be released to drive crack propagation (McClung, 1979; Heierli et al., 2008; Gaume et al., 2014b). On the other hand, with respect to the weak layer, a snowpack weakness is a prerequisite for failure initiation and offers a path for crack propagation. Sigrist and Schweizer (2007) were among the first to emphasize the importance of both the slab layers and the

The Cryosphere Discuss., doi:10.5194/tc-2016-84, 2016
Manuscript under review for journal The Cryosphere
Published: 18 April 2016

weak layer for crack propagation. Given the two most relevant processes in dry-snow slab avalanche release, failure initiation and crack propagation (e.g., Schweizer et al., 2003a), van Herwijnen and Jamieson (2007) suggested a conceptual model on the effect of the slab properties on these failure processes.

Temporal changes in snow instability hence may stem from changes in slab as well as weak layer properties – separately or in combination. For example, during a snowfall the probability of failure initiation in the weak layer increases due to the additional load. However, the additional load will also promote strengthening of the weak layer (e.g., Zeidler and Jamieson, 2006b) – though the strengthening may lag behind the loading. Whereas, changes of weak layer strength have been studied in detail (e.g., Jamieson and Johnston, 1999; Chalmers and Jamieson, 2001; Gauthier et al., 2010; Zeidler and Jamieson, 2006b, a), and more frequently than changes of slab properties, there are hardly any studies – to the best of our knowledge – that investigated how temporal changes affect the complex interplay between slab and weak layer properties.

Repeated measurements of the shear strength of weak layers revealed how various types of weak layers gain strength over time (Jamieson et al., 2007). In other words, almost exclusively, an increase in strength was observed in all studies – at the same time the load usually increased. Occasionally measured decreasing strength with time was attributed to spatial variability within the study site or errors associated with measurement technique (Jamieson and Johnston, 1999). Jamieson and Schweizer (2000) reported the shear strength over time for 19 buried surface hoar layers. Typical weak layer strength gain was on the order of 100 Pa d^{-1} during the initial weeks after burial (Schweizer et al., 1998).

Many of the above mentioned studies monitoring strength changes of weak layers focussed on the stability trends and associated avalanche activity (e.g., Jamieson et al., 2007). However, observed avalanche activity could often not be related to the stability index, the strength-to-stress approach, calculated from the study plot measurements. While the shear strength of the weak layer is important for failure initiation, dry-snow slab avalanches release due to crack propagation which requires the release of deformation energy stored in the slab layers. This conceptual mismatch has long been realized, for example, Schweizer et al. (1998) pointed out that since the shear frame measurements will primarily provide information on the strength and strength changes of weak layers, the ‘effective reactivity (propagation potential)’ depending on the slab characteristics should be assessed by supplementary tests. However, the temporal evolution of these slab characteristics was rarely monitored, apart of course, from the load.

The temporal evolution of the strength has been modelled for persistent and non-persistent weak layers (e.g., Chalmers, 2001; Zeidler and Jamieson, 2006b, a; Conway and Wilbour, 1999; Hayes et al., 2005; Lehning et al., 2004) so that the evolution of stability can be monitored or even forecasted. Conway and Wilbour (1999) suggested a model of natural snow stability during storms by comparing the load to the strength by assuming that failure occurs at the base of the new snow layers; their strength solely depends on density which increases with increasing overburden stress. Föhn and Hächler (1978) exclusively focused on slab properties as they studied how the slab layers settle during major snow storms. They proposed to follow the settlement (coefficient) over time to assess the probability of large spontaneously releasing dry-snow avalanches.

The Cryosphere Discuss., doi:10.5194/tc-2016-84, 2016
Manuscript under review for journal The Cryosphere
Published: 18 April 2016

With the propagation saw test (Gauthier and Jamieson, 2006) now a well-established snow stability test exists that provides a quantitative test result, the critical cut length, and allows determining the relevant slab and weak layer properties (Sigrist and Schweizer, 2007; van Herwijnen and Heierli, 2010; Schweizer et al., 2011; Reuter et al., 2015). Recently, Birkeland et al. (2014) repeatedly performed propagation saw tests on a layer of buried surface hoar; they focussed on conditions for fracture arrest.

A number of studies have focussed on the temporal evolution of spatial patterns on small uniform slopes – inter alia testing the hypothesis that variability should increase in the absence of major external forcing such as a snowfall (Birkeland and Landry, 2002; Birkeland et al., 2004; Logan et al., 2007). Hendrikx et al. (2009) focused on spatial variations of the propagation potential using the Extended Column Test (ECT) (Simenhois and Birkeland, 2009). They assessed the spatial variability of two sites each on two days and found increased spatial clustering on the second sampling day.

The aim of the present study is to repeatedly measure the slab and weak layer properties in a study plot to monitor their temporal evolution and to investigate their interaction in view of assessing snow instability. During the winter 2014-2015 we followed over the course of two months a layer of faceted crystals that was responsible for wide-spread avalanche activity in the region of Davos (Eastern Swiss Alps). We performed propagation saw tests, analysed them based on the video images taken during the tests and compared the results to the concurrently performed measurements of penetration resistance using the snow micro-penetrometer (SMP) (Schneebeli and Johnson, 1998). Hence, the acquired dataset provides a comprehensive time series of quantitative measures of snow instability; it allows insight into the complex interplay between slab and weak layer properties that jointly govern snow instability.

2 Methods

We followed the evolution of a weak layer of faceted crystals in the level study plot surrounding the automatic weather station WAN7 (2442 m a.s.l.) located in the Steintälli field site above Davos, eastern Swiss Alps (46.808° N, 9.788° E). Measurements were performed on eight days between 6 January and 3 March 2015, typically once a week during the two month study period (Table 1).

2.1 Weak layer formation and snowpack

On 1 December 2014 the manually observed snow profile at the study plot Weissfluhjoch (2540 m a.s.l.) (located 2.9 km to the northeast of WAN7) showed a melt-freeze layer with 1 cm recently fallen snow on top. On 2-3 December 2014, a minor storm accumulated 12 cm of new snow. During the following two weeks, this layer settled and transformed into a layer of faceted crystals due to near-surface faceting (Birkeland, 1998). The melt-freeze crust (2-3 cm in thickness) was consistently found throughout the winter below the layer of faceted crystals that ultimately formed the weak layer (5-8 cm in thickness). As of mid January 2015 the layer was classified as rounded facets (FCxr), grain size about 1-1.5 mm. Above the weak layer of faceted crystals was another layer of facets overlain by well consolidated slab layers that had formed in late December

The Cryosphere Discuss., doi:10.5194/tc-2016-84, 2016
Manuscript under review for journal The Cryosphere
Published: 18 April 2016

2014 and early January 2015. The weak layer was likely responsible for wide-spread avalanche activity in the region of Davos on 30-31 December 2014. While no fracture line profiles were observed to provide hard evidence, the layer consistently failed in snow stability tests in early January 2015.

2.2 Field measurements

On each of the eight sampling days we observed a manual snow profile, including layer density, according to Fierz et al. (2009). The detailed density profile is required for the analysis by particle tracking velocimetry (PTV) of the PSTs (see below). The manual snow profile served as reference for most other measurements and was completed with the two snow instability tests that can easily be performed in flat terrain: the compression test (CT) (Jamieson, 1999) and the extended column test (ECT) (Simenhois and Birkeland, 2009).

On each sampling day, except for 19 February 2015, we also conducted at least three propagation saw tests (PST) within 2 meters of the snow profile location. The tests were performed according to Greene et al. (2010), albeit with longer columns. Initially, column length was around 1.5 m, and it increased towards 2 m at the end of the study period as the weak layer was buried more deeply (slab thickness increased from 59 to 148 cm) (Bair et al., 2014; Gaume et al., 2015). Using a 2-mm thick snow saw, we cut the layer of faceted crystals at its upper interface, where CT and ECT results indicated the failure to occur. In some cases a test result had to be discarded since the cut was not performed consistently close to the interface. Black markers (2.5 cm in diameter) were inserted into the snowpack; we filmed all tests with a high speed video camera for subsequent analysis by particle tracking velocimetry (van Herwijnen et al., 2010).

Concurrently, we performed several SMP measurements, at least three at the location of the manual snow profile, and at least one at each of the PST locations; thus in total at least 6 measurements per sampling day. The SMP measurements at the PST locations were conducted before isolating the columns, close to the end of the column where the saw cut was initiated. This procedure allowed a one-by-one comparison of the SMP-derived properties with those from the PTV analysis.

2.3 PTV analysis

Based on the bending of the slab due to the saw cut (of length r) during the PST, the bulk effective modulus of the slab E^{*PTV} and the specific fracture energy of the weak layer w_f^{PTV} were determined as outlined in van Herwijnen and Heierli (2010). In short, the displacement of the markers was used to estimate the mechanical energy $V_m(r)$ with increasing crack length. The measured mechanical energy was then fitted to an analytical expression for $V_m(r)$ (Heierli, 2008) to obtain the bulk effective modulus (which is the fit parameter). To determine the specific fracture energy, the analytical expression for the mechanical energy with the best fit modulus, is differentiated with regard to the crack length at the critical cut length r_c^{OBS}. In other words, the slope of $V_m(r)$ at the critical crack length corresponds to the specific fracture energy of the weak layer. For a more detailed description on deriving the bulk effective modulus and the specific fracture energy, the reader is referred to van Herwijnen and Heierli (2010). In addition, the video analysis allowed to accurately determine the critical value of the crack length, when the crack started to propagate.

The Cryosphere Discuss., doi:10.5194/tc-2016-84, 2016
Manuscript under review for journal The Cryosphere
Published: 18 April 2016

2.4 SMP signal processing

We used the penetration resistance data acquired with the SMP to obtain detailed data on the layering of the snow cover, including layer densities (Proksch et al., 2015), and thus also the load on the weak layer. Based on the manually observed snow profile layers were manually defined from the corresponding sections of the SMP signals (Reuter et al., 2015). The micro-mechanical effective modulus for the slab layers and the strength of the weak layer were calculated according to Johnson and Schneebeli (1999), whereas the weak layer specific fracture energy was derived as suggested by Reuter et al. (2013). Based on the detailed layering of the slab, the effective bulk modulus of the slab was determined with the help of a finite element (FE) model of the experimental setup (for details see Reuter et al., 2015). The SMP-derived weak layer fracture energy and the bulk modulus were adjusted by a linear factor of 2.7 and 2.2, respectively, to match the corresponding values derived from the PTV analysis. Scaling of the specific fracture energy and the modulus seems justified as there is no calibration yet of the microstructural mechanical properties that can be derived from the SMP signal.

Furthermore, two metrics of point instability, namely the failure initiation criterion S and the crack propagation criterion r_c^{SMP} (SMP-derived critical cut length), were derived from the SMP data as suggested by Reuter et al. (2015). All the procedures to obtain the above mentioned mechanical properties are described in detail in Reuter et al. (2015).

2.5 Snow cover modelling

We compared the results of the field measurements to output of the numerical snow cover model SNOWPACK (e.g., Lehning et al., 2004) driven by meteorological input from the automatic weather station WAN7. In particular, we evaluated the skier stability index SK38 as introduced by Jamieson and Johnston (1998). In addition, we made an attempt to calculate the critical cut length r_c^{SNP} from the detailed snow stratigraphy provided by SNOWPACK. In analogy to the calculation of the critical cut length from SMP-derived parameters (see section above), we followed the same procedure, but used SNOWPACK model output to derive all the required mechanical properties of the snow layers. The critical cut length was estimated based on the relation given by Gaume et al. (2014a, Eq. 5) (see Gaume et al., 2016 for a detailed derivation). Based on discrete element modelling they suggested the critical cut length, in the flat (for slope angle $\psi = 0°$), to essentially be depending on the slab modulus, the slab load σ_n, and the weak layer shear strength τ_s :

$$r_c^{SNP} = \Lambda \sqrt{\frac{2\,\tau_s}{\sigma_n}} \qquad (1)$$

with $\Lambda = (E'\,h\,h_{WL}/G_{WL})^{1/2}$ where $E' = E/(1-\nu^2)$ is the slab modulus with ν the Poisson's ratio, h the slab thickness, and h_{WL} the thickness and G_{WL} the shear modulus of the weak layer. All the required parameters are provided by SNOWPACK, except for the shear modulus of the weak layer which was estimated. For the slab modulus we used the bulk modulus rather than the average modulus. Following the procedure described by Reuter et al. (2015) the elastic moduli of the slab layers were derived from density using the relation provided by Scapozza (2004, p. 186). With these properties

The Cryosphere Discuss., doi:10.5194/tc-2016-84, 2016
Manuscript under review for journal The Cryosphere
Published: 18 April 2016

(modulus, layer density and thickness) a FE simulation was performed to determine the bulk modulus, i.e. we followed the same procedure as for the SMP-derived bulk modulus.

2.6 Avalanche activity

For validation purposes we refer to avalanches observed during the winter 2014-2015 in the region of Davos. Based on detailed observations of the number, type and size of avalanches by personnel from the local ski areas, the avalanche warning service, SLF staff members, and others, the avalanche activity index per day as described by Schweizer et al. (2003b) was calculated. The index is a weighted sum of the number of observed avalanches per day including spontaneously releasing as well as artificially triggered avalanches; the weights depend on the avalanche size and are 0.01, 0.1, 1 and 10 for Canadian size classes 1 to 4, respectively (McClung and Schaerer, 2006).

2.7 Sensitivity study

To explore the complex interaction between slab and weak layer properties on the critical cut length in a PST, we explored the theoretical expression, based on the work by Heierli (2008), linking the specific fracture energy of the weak layer, the elastic modulus, the density and the thickness of the slab with the critical crack length for a self-propagating crack:

$$w_f(E, r_c) = \frac{h}{2E}\left[w_0 + w_1\frac{r_c}{h} + w_2\left(\frac{r_c}{h}\right)^2 + w_3\left(\frac{r_c}{h}\right)^3 + w_4\left(\frac{r_c}{h}\right)^4\right] \quad . \qquad (2)$$

For various scenarios of the temporal evolution of load (slab density and thickness), slab modulus, and weak layer specific fracture energy, we calculated the corresponding crack length by numerically solving Eq. (2). For details on Eq. 2 the reader is referred to Schweizer et al. (2011) where the above theoretical expression is Eq. 4, and Eqs. 5-9.

3 Results

3.1 Propagation saw test results

On 6 January 2015, when we did the first propagation saw tests, cracks did not always fully propagate to the end of the column, and slab fractures were also observed (Figure 1a). On 14 January 2015, when the PSTs were performed on a slightly more shallow part of the study plot surrounding the automatic weather station WAN7, all tests resulted in slab fractures. As of 28 January 2015, all PSTs resulted in full propagations to the end of the column. On 3 March 2015, we did the last tests; in all three tests the crack fully propagated to the end; the critical crack length was about 50 cm. By then, the weak layer of faceted crystals was buried below a slab of about 150 cm in thickness with an average density of about 270 kg m^{-3}, resulting in a load of almost 4 kPa.

Initially, the critical cut length was about 23-30 cm, and slightly increased up to 21 January 2015. Consistently short cut lengths were observed on the following measurement day, on 28 January 2015, the date when all cracks for the first time

The Cryosphere Discuss., doi:10.5194/tc-2016-84, 2016
Manuscript under review for journal The Cryosphere
Published: 18 April 2016

propagated to the very end of the column. On the following sampling day, 3 February 2015, one test again yielded a short cut length, 17 cm, the shortest value recorded during our sampling period. Subsequently, the cut lengths increased with time.

In summary, the PST results suggest that the temporal evolution of the critical cut length showed a minimum between the end of January and the beginning of February. In other words, the crack propagation propensity did initially, in early and mid January slightly decrease, then increased as indicated by the lowest values of the critical cut length at the end of January and the beginning of February, and subsequently decreased towards the end of the sampling period.

3.2 Load

The weak layer was initially, on 6 January 2015, buried below a slab of 59 cm at a height of 56 cm (total snow depth HS: 115 cm); the initial load was about 1.4 kPa (Table 1, Figure 1b). The load did not change much during the following week but then continuously increased due to snowfalls to almost 3 kPa by early February 2015. After a fair weather period in February with no new snow for more than two weeks, the snow depth increased again and on the last sampling day (3 March 2015) the load was about 3.9 kPa.

The density derived from the SMP signal agreed well with the manually measured density and accordingly the temporal evolution of the load above the weak layer was well represented with the SMP measurements (Figure 1b).

For comparison, also the load as calculated from average density and slab thickness provided by the numerical snow cover model SNOWPACK is shown. Initial and final values of load were about similar whereas in-between the load provided by SNOWPACK rather underestimated the observed load. The underestimation is mainly due to the fact that the modelled snow depth is about 25 cm lower than the observed one.

3.3 Effective bulk modulus of the slab

The effective bulk modulus of the slab was derived from the bending of the slab during the propagation saw test via the PTV analysis as well as from the SMP signal analysis using the FE model (Figure 2). The values obtained from the PTV analysis suggest that overall the modulus increased from about 2 to 8 MPa during the two-month sampling period. The SMP analysis, on the other hand, reveals that the modulus did not change much but stayed about the same with time; the initial and the last values were about 1.5 MPa.

3.4 WL specific fracture energy

The PTV analysis suggests that the specific fracture energy increased with time from about 0.8 J m^{-2} to about 2.3 J m^{-2}, with almost no increase during the first half of the period, but with a significant increase after the end of January 2015 (Figure 3a). The SMP analysis revealed a similar trend of increasing weak layer fracture energy with time. The specific fracture energy increased from about 0.3 J m^{-2} to about 1.5 J m^{-2}; i.e. it particularly increased towards the end of February (Figure 3b).

The Cryosphere Discuss., doi:10.5194/tc-2016-84, 2016
Manuscript under review for journal The Cryosphere
Published: 18 April 2016

3.5 SMP metrics of instability

The failure initiation criterion *S* calculated from the SMP resistance profile was initially about 300 to 500 indicating a rather low initiation probability given the threshold reported by Reuter et al. (2015). They observed that a value of about 230 divided between the cases with and without concurrently observed signs of instability. The index then increased towards the end of January to about 1000-1500 and stayed high until the end of the sampling period (Figure 4a). The SMP-derived failure propagation criterion r_c^{SMP} was about 18 cm at the beginning of January, and then decreased, and was lowest in early February. Subsequently, it slightly increased again towards the end of the sampling period (Figure 4b).

3.6 Snow cover modelling: SNOWPACK output

Figures 4c and 4d show the instability output from the numerical snow cover model SNOWPACK calculated for the location of the automatic weather station WAN7. The skier stability index SK38 (Figure 4c) had values below one in early January 2015 and then increased towards the end of January to about 1.2-1.3, and stayed at that level during the rest of the sampling period. The modelled critical cut length r_c^{SNP} (Figure 4d) based on Eq. 1 and FE simulations using the detailed snow stratigraphy provided by SNOWPACK almost steadily increased from about 15 cm to 60 cm.

3.7 Avalanche activity

The highest avalanche activity in the region of Davos was observed around the end of the year 2014 (Figure 5). In January 2015, avalanches were occasionally observed, in particular on 18 January, a sunny Sunday after a snowfall. Again towards late January and early February, there was some increased activity. The last peak was on 3 March 2015, again after a major snowfall, but during this period avalanches did no longer run on the weak layer of facets we monitored. Overall, it seems that the avalanche release probability clearly decreased since early January 2015, but whenever there was a significant snowfall in late January so that the slab changed due to the additional load some avalanches were again observed (e.g. on 18, 28 and 31 January, Figure 5), i.e. the weak layer of facets was still reactive, a true persistent weak layer.

The decreasing trend of triggering probability is in line with the observed results of the CTs and ECTs we performed concurrently on each of the sampling days. The scores increased from values just below 20 taps to values of around 30 taps (Figure 5).

3.8 Sensitivity of critical crack length

Given the observed temporal evolution of the critical cut length (increasing, decreasing and then increasing values) in our PSTs, we explored the sensitivity of the critical cut length to evaluate the conditions for increasing or decreasing cut length as a function of the specific fracture energy of the weak layer w_f, the load σ_n and the modulus of the slab *E*.

In the first simplified scenario of temporal evolution, all the parameters (w_f, σ_n and *E*) were assumed to increase. This corresponds to a situation when the slab gets thicker and stiffer, and the weak layer simultaneously gains strength due to

The Cryosphere Discuss., doi:10.5194/tc-2016-84, 2016
Manuscript under review for journal The Cryosphere
Published: 18 April 2016

the increased load. Consequently, the critical cut length did almost not change (or increased very slightly only) (Figures 6a,b). The combination of increasing load, but also increasing slab stiffness provided a bit more energy to drive the crack, but just as much about to compensate the increased specific fracture energy of the slab.

In the second simplified scenario (Figures 6c,d) the specific fracture energy increased as the load increased, but the slab modulus was assumed not to change. The slab modulus may not change, even if the thickness increases, if the slab is dominated, for example, by a strong thick crust. This scenario resulted in a decrease of the critical cut length. Due to the higher load, more energy was available to drive the crack; obviously, even with increasing specific fracture energy this effect dominated.

In third simplified scenario (Figures 6e,f) the load stayed constant, as in a fair weather period, but the stiffness increased (due to settlement), and the weak layer fracture energy also slightly increased, i.e. the layer gained strength, for example, due to ongoing sintering with increasing age. In this scenario, the critical cut length considerably increased. Due to the higher stiffness less energy could be released to drive crack propagation and at the same time the weak layer became tougher.

Finally, we tried to roughly mimic the temporal evolution of the critical cut length as observed in our PSTs. We assumed the load to increase as observed, the stiffness to triple during the sampling period (as derived from the PTV analysis) and the specific fracture energy of the weak layer to increase as well, but not continuously. In fact, it was possible to obtain a temporal evolution of the critical cut length that had a local minimum about in the middle of the sampling period (Figures 6g,h).

Alternatively, Eq. (1) could be used to explore the sensitivity of the critical cut length. In fact, this would reveal the same trends for the critical cut length if the temporal evolution of the shear strength follows the one assumed for the critical cut length.

4 Discussion

We followed the temporal evolution of a weak layer of faceted crystals applying state-of-the-art measurement techniques, namely particle tracking velocimetry to evaluate the propagation saw tests and the snow micro-penetrometer, to assess its failure initiation and, in particular, its crack propagation propensity.

While performing the propagation saw tests in the study plot, we initially observed a mixture of END and SF test results. Only when the load had reached 2 kPa, all cracks fully propagated towards the end of the column. This finding suggests that the slab was initially not strong enough to support the propagation (Gaume et al., 2015), in particular at the more shallow locations – which is in contrast to the avalanche activity that was observed during this time. The contrasting observations may be due to the fact that the slab might have been stronger in typical lee-slope starting zones – indicating some of the limitations when extrapolating instability from flat field study sites.

The Cryosphere Discuss., doi:10.5194/tc-2016-84, 2016
Manuscript under review for journal The Cryosphere
Published: 18 April 2016

The critical cut length as observed in the PSTs showed a distinct temporal evolution suggesting that the crack propagation propensity was highest around the middle of the sampling period (late January/early February). This pattern of the temporal evolution of the critical cut length in PSTs was not expected. Though the PST results may be influenced by some small scale spatial variability of the snowpack in the study plot, we deem it unlikely that the observed pattern is entirely the result of spatial variability and does not reflect the temporal evolution. Furthermore, the high propagation propensity observed in late January/early February coincides with increased avalanche activity (Figure 5). The median range of the PST results on a given sampling day was 5.9 cm, so that the resulting uncertainty in the mean is about 2-3 cm. Reuter and Schweizer (2012) reported a standard deviation of the critical cut length on days with surface warming of about 5 cm. Similar variations for PST results on a single day at a single location have been reported by Gauthier and Jamieson (2008). Previous studies performed in level study plots have shown that measurements in general are reliable and that the effect of spatial variations is relatively small. Jamieson (1995) reported a mean coefficient of variation of shear strength of about 15% for sets of measurements in study plots. Correspondingly, variations in stability indices derived from study plot measurements of load and shear strength, two measurements that have comparable errors as the PST, were found to be indicative of avalanche activity (e.g., Jamieson et al., 2007).

The errors associated with the parameters derived from the PTV analysis (i.e. the measurement uncertainty) were about 23% (or about 1 MPa) for the modulus and about 12% (or about 0.1 J/m^2) for the weak layer specific fracture energy. These estimates are based on calculating these properties 1000 times for each experiment accounting for the uncertainty in the input parameters (uncertainty in the distance measurements in the field, density measurements, and especially the location estimates of the dots in the PTV analysis). Comparison with Figures 2 and 3 shows that the spread found in side by side experiments on a single day is often smaller than the measurements uncertainty for the modulus, but less so for the weak layer fracture energy. This suggests that the reproducibility for the values of the slab stiffness is good (even though they have greater uncertainty), whereas the reproducibility for the weak layer fracture energy was some lower.

The errors of the SMP-derived parameters are more difficult to assess. However, Proksch et al. (2015) have shown that in particular the SMP-derived density is a reliable measure. Their finding is supported by our measurements that showed a good reproducibility between SMP-derived load and manually measured load (Figure 1b). Also, the two SMP-derived metrics of instability were validated with independent observations of instability (Reuter et al., 2015). However, it seems that in particular the derivation of the effective elastic modulus is more prone to errors.

Apart from the effective modulus, the other parameters derived with the two independent methods (PTV and SMP) showed very similar temporal evolution – although the absolute values may differ. The latter finding is known (e.g., Reuter et al., 2013), and both the effective slab modulus as well as the specific fracture energy of the weak layer have to be considered as relative values rather than absolute ones. In the case of the PTV analysis, the stiffness of the slab is likely to include some non-elastic parts of deformation, thereby increasing the specific fracture energy to values that are occasionally larger than the specific fracture energy of ice which seems unrealistic (McClung, 2015).

The Cryosphere Discuss., doi:10.5194/tc-2016-84, 2016
Manuscript under review for journal The Cryosphere
Published: 18 April 2016

The SMP metrics of instability suggested that failure initiation became increasingly hard during the sampling period, whereas crack propagation propensity even increased or at least stayed very high. The suggested trend in failure initiation is in line with the observations, in particular when considering the CT and ECT scores. On the other hand, the temporal evolution of the critical cut length as observed with PSTs could not be reproduced; though there was a slight minimum in early February for the SMP-derived metric, roughly around the middle of the sampling period.

A different temporal behaviour was observed for two corresponding metrics of instability provided by SNOWPACK. Whereas the skier stability index in general increased during the first weeks, it stayed at a level of about 1.2-1.3 for the remainder of the sampling period – a value that seems low given the observation that triggering became increasingly hard. The propagation propensity metric, the modelled critical cut length r_c^{SNP}, steadily increased during the sampling period – suggesting that the propagation propensity decreased. This behaviour follows from the fact that two of the essential variables, the bulk modulus and the weak layer shear strength also increase with time. In particular, the shear strength increases with increasing density of the weak layer – though persistent weak layers are known to hardly settle despite increasing overburden pressure due to their anisotropic microstructure (e.g., Walters and Adams, 2014; Reiweger and Schweizer, 2010). However, it seems premature to rate this metric as it has to be considered as being still in an experimental state.

Finally, the simple sensitivity study varying the slab load and modulus, and the specific fracture energy of the weak layer to explore the effect on the critical cut length shed some light on the interaction of the various parameters and the consequences for snow instability assessment. It helps to understand, for example, how changes in slab properties may affect the propagation propensity. The parameter most strongly influencing the critical cut length seems to be the load. Even with an increasing weak layer fracture energy the increasing load caused the cut length to decrease (Figures 6c,d). This consistent decrease was however not observed in our case. There was only a decrease initially and then a clear increase towards the end of the measurement period – suggesting that the increase in slab stiffness and/or specific fracture energy (over)-compensated the effect of the increasing load. The final, more or less realistic scenario, should by no means be seen as a validation of the observed temporal evolution of critical cut length, but simply shows that it is entirely possible that under certain conditions the cut length may increase or decrease in the course of time, primarily due to changes of slab properties. Exploring Eq. 1 relating slab modulus and load, and weak layer shear strength provided very similar results (not shown) confirming the findings of the sensitivity study.

5 Conclusions

We have monitored the temporal evolution of a weak layer of faceted crystals that was one of the critical weaknesses during the winter 2014-2015 in the region of Davos (Eastern Swiss Alps). We focused on the crack propagation propensity and performed propagation saw tests on seven sampling days during a two-month period from early January to early March 2015. Tests were completed with objective measurements, namely by resistance profiles acquired with the snow micro-

penetrometer and particle tracking velocimetry based on video images of the PSTs. Our dataset represents to the best of our knowledge the first comprehensive time series of quantitative measures of snow instability.

The critical cut length, observed in the PSTs, showed a distinct pattern of temporal evolution: initially increasing, then decreasing with a minimum around the end of January/early February, and subsequently increasing again towards the end of the sampling period.

The relevant mechanical properties, either determined by PTV analysis or derived from the SMP signal, namely the slab stiffness and weak layer fracture energy, in general increased, or in the case of the SMP-derived modulus showed no distinct temporal trend. These findings suggest that it is not possible to assess crack propagation propensity by simply monitoring some of the relevant mechanical properties. One has to consider the complex interaction between the stiffness and load of the slab, and the weak layer fracture energy.

Traditional and newly-developed metrics of snow instability describing either the failure initiation or the crack propagation propensity, calculated from simulated snow stratigraphy (SNOWPACK) or derived from the SMP signal, did partially reproduce the observed temporal pattern. Whereas the initiation indices appropriately indicated that triggering probability decreased, the predictions for the critical length were less in line with the observed temporal pattern.

Whereas the PST combined with the PTV approach seems to provide the most reliable measure of propagation propensity and corresponding mechanical properties, the procedure is time consuming. However, this disadvantage can only be outweighed, if modelled metrics of instability become more reliable which will require further validation studies and possibly an enhancement of the representation of mechanical properties in the model.

Acknowledgments

We are grateful to Franziska Zahner and Achille Capelli for help with the field work. Frank Techel provided the avalanche activity data. B. Reuter has been supported by a grant of the Swiss National Science Foundation (200021_144392) and J. Gaume by a Swiss Government Excellence Scholarship and is grateful to the State Secretariat for Education, Research and Innovation SERI of the Swiss Government.

The Cryosphere Discuss., doi:10.5194/tc-2016-84, 2016
Manuscript under review for journal The Cryosphere
Published: 18 April 2016

References

Bair, E. H., Simenhois, R., van Herwijnen, A., and Birkeland, K.: The influence of edge effects on crack propagation in snow stability tests, Cryosphere, 8, 1407-1418, 10.5194/tc-8-1407-2014, 2014.

Birkeland, K., and Landry, C.: Changes in spatial patterns of snow stability through time, Proceedings ISSW 2002. International Snow Science Workshop, Penticton BC, Canada, 29 September-4 October 2002, 482-490, 2002.

Birkeland, K., Kronholm, K., Schneebeli, M., and Pielmeier, C.: Changes in shear strength and micropenetration hardness of a buried surface-hoar layer, Ann. Glaciol., 38, 223-228, 10.3189/172756404781815167, 2004.

Birkeland, K. W.: Terminology and predominant processes associated with the formation of weak layers of near-surface faceted crystals in the mountain snowpack, Arctic and Alpine Research, 30, 193-199, 1998.

Birkeland, K. W., van Herwijnen, A., Knoff, E., Staples, M., Bair, E. H., and Simenhois, R.: The role of slabs and weak layers in fracture arrest, Proceedings ISSW 2014. International Snow Science Workshop, Banff, Alberta, Canada, 29 September - 3 October 2014, 156-168, 2014.

Chalmers, T. S.: Forecasting shear strength and skier-triggered avalanches for buried surface hoar layers, Faculty of Graduate Studies, University of Calgary, Calgary AB, Canada, 107 pp., 2001.

Chalmers, T. S., and Jamieson, J. B.: Extrapolating the skier stability of buried surface hoar layers from study plot measurements, Cold Reg. Sci. Technol., 33, 163-177, 10.1016/S0165-232X(01)00043-X, 2001.

Conway, H., and Wilbour, C.: Evolution of snow slope stability during storms, Cold Reg. Sci. Technol., 30, 67-77, 10.1016/S0165-232X(99)00009-9, 1999.

Fierz, C., Armstrong, R. L., Durand , Y., Etchevers, P., Greene, E., McClung, D. M., Nishimura, K., Satyawali, P. K., and Sokratov, S. A.: The International Classification for Seasonal Snow on the Ground, HP-VII Technical Documents in Hydrology, IACS Contribution No 1, UNESCO-IHP, Paris, France, 90 pp., 2009.

Föhn, P., and Hächler, P.: Prévision de grosses avalanches au moyen d'un modèle déterministe-statistique, Comptes Rendues de la Deuxième Rencontre Internationale sur la Neige et les Avalanches, Grenoble, France, 12-14 avril 1978, 151-165, 1978.

Gaume, J., Chambon, G., Reiweger, I., van Herwijnen, A., and Schweizer, J.: On the failure criterion of weak-snow layers using the discrete element method, Proceedings ISSW 2014. International Snow Science Workshop, Banff, Alberta, Canada, 29 September - 3 October 2014, 681-688, 2014a.

Gaume, J., Schweizer, J., van Herwijnen, A., Chambon, G., Reuter, B., Eckert, N., and Naaim, M.: Evaluation of slope stability with respect to snowpack spatial variability, J. Geophys. Res., 119, 1783-1799, 10.1002/2014JF00319, 2014b.

Gaume, J., van Herwijnen, A., Chambon, G., Birkeland, K. W., and Schweizer, J.: Modeling of crack propagation in weak snowpack layers using the discrete element method, Cryosphere, 9, 1915-1932, 10.5194/tc-9-1915-2015, 2015.

Gaume, J., van Herwijnen, A., Chambon, G., Wever, N., and Schweizer, J.: Snow fracture in relation to slab avalanche release: critical state for the onset of crack propagation, Cryosphere Discuss., 10.5194/tc-2016-64, in review, 2016.

Gauthier, D., and Jamieson, J. B.: Evaluating a prototype field test for weak layer fracture and failure propagation, Proceedings ISSW 2006. International Snow Science Workshop, Telluride CO, U.S.A., 1-6 October 2006, 107-116, 2006.

Gauthier, D., and Jamieson, B.: Evaluation of a prototype field test for fracture and failure propagation propensity in weak snowpack layers, Cold Reg. Sci. Technol., 51, 87-97, 10.1016/j.coldregions.2007.04.005, 2008.

Gauthier, D., Brown, C., and Jamieson, B.: Modeling strength and stability in storm snow for slab avalanche forecasting, Cold Reg. Sci. Technol., 62, 107-118, 10.1016/j.coldregions.2010.04.004, 2010.

Greene, E., Atkins, D., Birkeland, K., Elder, K., Landry, C., Lazar, B., McCammon, I., Moore, M., Sharaf, D., Sterbenz, C., Tremper, B., and Williams, K.: Snow, Weather and Avalanches: Observational Guidelines for Avalanche Programs in the United States, 2nd ed., American Avalanche Association (AAA), Pagosa Springs CO, U.S.A., 152 pp., 2010.

Habermann, M., Schweizer, J., and Jamieson, J. B.: Influence of snowpack layering on human-triggered snow slab avalanche release, Cold Reg. Sci. Technol., 54, 176-182, 10.1016/j.coldregions.2008.05.003, 2008.

Hayes, P., Wilbour, C., Gibson, R., Marshall, H. P., and Conway, H.: A simple model of snow slope stability during storms, Proceedings ISSW 2004. International Snow Science Workshop, Jackson Hole WY, U.S.A., 19-24 September 2004, 165-171, 2005.

Heierli, J.: Anticrack model for slab avalanche release, Ph.D., University of Karlsruhe, Karlsruhe, Germany, 102 pp., 2008.

Heierli, J., Gumbsch, P., and Zaiser, M.: Anticrack nucleation as triggering mechanism for snow slab avalanches, Science, 321, 240-243, 10.1126/science.1153948, 2008.

Hendrikx, J., Birkeland, K., and Clark, M.: Assessing changes in the spatial variability of the snowpack fracture propagation propensity over time, Cold Reg. Sci. Technol., 56, 152-160, 10.1016/j.coldregions.2008.12.001, 2009.

Jamieson, B., and Johnston, C. D.: Snowpack factors associated with strength changes of buried surface hoar layers, Cold Reg. Sci. Technol., 30, 19-34, 10.1016/S0165-232X(99)00026-9, 1999.

Jamieson, J. B.: Avalanche prediction for persistent snow slabs, Department of Civil Engineering, University of Calgary, Calgary AB, Canada, 258 pp., 1995.

Jamieson, J. B., and Johnston, C. D.: Refinements to the stability index for skier-triggered dry slab avalanches, Ann. Glaciol., 26, 296-302, 1998.

Jamieson, J. B.: The compression test - after 25 years, The Avalanche Review, 18, 10-12, 1999.

Jamieson, J. B., and Schweizer, J.: Texture and strength changes of buried surface hoar layers with implications for dry snow-slab avalanche release, J. Glaciol., 46, 151-160, 10.3189/172756500781833278, 2000.

Jamieson, J. B., Zeidler, A., and Brown, C.: Explanation and limitations of study plot stability indices for forecasting dry snow slab avalanches in surrounding terrain, Cold Reg. Sci. Technol., 50, 23-34, 10.1016/j.coldregions.2007.02.010, 2007.

Johnson, J. B., and Schneebeli, M.: Characterizing the microstructural and micromechanical properties of snow, Cold Reg. Sci. Technol., 30, 91-100, 10.1016/S0165-232X(99)00013-0, 1999.

Lehning, M., Fierz, C., Brown, R. L., and Jamieson, J. B.: Modeling instability for the snow cover model SNOWPACK, Ann. Glaciol., 38, 331-338, 10.3189/172756404781815220, 2004.

Logan, S., Birkeland, K. W., Kronholm, K., and Hansen, K. J.: Temporal changes in the slope-scale spatial variability of the shear strength of buried surface hoar layers, Cold Reg. Sci. Technol., 47, 148-158, 10.1016/j.coldregions.2006.08.002, 2007.

McClung, D. M.: Shear fracture precipitated by strain softening as a mechanism of dry slab avalanche release, J. Geophys. Res., 84, 3519-3526, 1979.

McClung, D. M., and Schaerer, P.: The Avalanche Handbook, 3rd ed., The Mountaineers Books, Seattle WA, U.S.A., 342 pp., 2006.

McClung, D. M.: Mode II fracture parameters of dry snow slab avalanche weak layers calculated from the cohesive crack model, Int. J. Fracture, 193, 153-169, 10.1007/s10704-015-0026-1, 2015.

Monti, F., Gaume, J., van Herwijnen, A., and Schweizer, J.: Snow instability evaluation: calculating the skier-induced stress in a multi-layered snowpack, Nat. Hazards Earth Syst. Sci., 16, 775-788, 10.5194/nhess-16-775-2016, 2016.

Proksch, M., Löwe, H., and Schneebeli, M.: Density, specific surface area and correlation length of snow measured by high-resolution penetrometry, J. Geophys. Res., 120, 346-362, 10.1002/2014JF003266, 2015.

Reiweger, I., and Schweizer, J.: Failure of a layer of buried surface hoar, Geophys. Res. Lett., 37, L24501, 10.1029/2010GL045433, 2010.

Reuter, B., and Schweizer, J.: The effect of surface warming on slab stiffness and the fracture behavior of snow, Cold Reg. Sci. Technol., 83-84, 30-36, 10.1016/j.coldregions.2012.06.001, 2012.

Reuter, B., Proksch, M., Löwe, H., van Herwijnen, A., and Schweizer, J.: On how to measure snow mechanical properties relevant to slab avalanche release, Proceedings ISSW 2013. International Snow Science Workshop, Grenoble, France, 7-11 October 2013, 7-11, 2013.

Reuter, B., Schweizer, J., and van Herwijnen, A.: A process-based approach to estimate point snow instability, Cryosphere, 9, 837-847, 10.5194/tc-9-837-2015, 2015.

Scapozza, C.: Entwicklung eines dichte- und temperaturabhängigen Stoffgesetzes zur Beschreibung des visko-elastischen Verhaltens von Schnee, Institut für Geotechnik, ETH Zurich, Zurich, Switzerland, 250 pp., 2004.

Schneebeli, M., and Johnson, J. B.: A constant-speed penetrometer for high-resolution snow stratigraphy, Ann. Glaciol., 26, 107-111, 1998.

Schweizer, J., Jamieson, J. B., and Skjonsberg, D.: Avalanche forecasting for transportation corridor and backcountry in Glacier National Park (BC, Canada), in: 25 Years of Snow Avalanche Research, Voss, Norway, 12-16 May 1998, edited by: Hestnes, E., NGI Publication, Norwegian Geotechnical Institute, Oslo, Norway, 238-243, 1998.

Schweizer, J., Jamieson, J. B., and Schneebeli, M.: Snow avalanche formation, Rev. Geophys., 41, 1016, 10.1029/2002RG000123, 2003a.

Schweizer, J., Kronholm, K., and Wiesinger, T.: Verification of regional snowpack stability and avalanche danger, Cold Reg. Sci. Technol., 37, 277-288, 10.1016/S0165-232X(03)00070-3, 2003b.

Schweizer, J., van Herwijnen, A., and Reuter, B.: Measurements of weak layer fracture energy, Cold Reg. Sci. Technol., 69, 139-144, 10.1016/j.coldregions.2011.06.004, 2011.

Sigrist, C., and Schweizer, J.: Critical energy release rates of weak snowpack layers determined in field experiments, Geophys. Res. Lett., 34, L03502, 10.1029/2006GL028576, 2007.

Simenhois, R., and Birkeland, K. W.: The Extended Column Test: Test effectiveness, spatial variability, and comparison with the Propagation Saw Test, Cold Reg. Sci. Technol., 59, 210-216, 2009.

Thumlert, S., and Jamieson, B.: Stress measurements in the snow cover below localized dynamic loads, Cold Reg. Sci. Technol., 106-107, 28-35, 10.1016/j.coldregions.2014.06.002, 2014.

van Herwijnen, A., and Jamieson, J. B.: Snowpack properties associated with fracture initiation and propagation resulting in skier-triggered dry snow slab avalanches, Cold Reg. Sci. Technol., 50, 13-22, 10.1016/j.coldregions.2007.02.004, 2007.

van Herwijnen, A., and Heierli, J.: A field method for measuring slab stiffness and weak layer fracture energy, International Snow Science Workshop ISSW, Lake Tahoe CA, U.S.A., 17-22 October 2010, 232-237, 2010.

van Herwijnen, A., Schweizer, J., and Heierli, J.: Measurement of the deformation field associated with fracture propagation in weak snowpack layers, J. Geophys. Res., 115, F03042, 10.1029/2009JF001515, 2010.

Walters, D. J., and Adams, E. E.: Quantifying anisotropy from experimental testing of radiation recrystallized snow layers, Cold Reg. Sci. Technol., 97, 72-80, 10.1016/j.coldregions.2013.09.014, 2014.

Zeidler, A., and Jamieson, J. B.: Refinements of empirical models to forecast the shear strength of persistent weak snow layers: PART B: Layers of surface hoar crystals, Cold Reg. Sci. Technol., 44, 184-193, 10.1016/j.coldregions.2005.11.004, 2006a.

The Cryosphere Discuss., doi:10.5194/tc-2016-84, 2016
Manuscript under review for journal The Cryosphere
Published: 18 April 2016

Zeidler, A., and Jamieson, J. B.: Refinements of empirical models to forecast the shear strength of persistent weak snow layers PART A: Layers of faceted crystals, Cold Reg. Sci. Technol., 44, 194-205, 10.1016/j.coldregions.2005.11.005, 2006b.

The Cryosphere Discuss., doi:10.5194/tc-2016-84, 2016
Manuscript under review for journal The Cryosphere
Published: 18 April 2016

Tables

Table 1: Snowpack characteristics on the eight measurements days.

Date	Snow depth (cm)	Slab thickness (cm)	Slab density (kg m^{-3})	Load (kPa)
06 Jan 2015	115	59	245	1.42
14 Jan 2015	110	56	272	1.50
21 Jan 2015	126	72	275	1.94
28 Jan 2015	161	108	207	2.20
03 Feb 2015	172	117	242	2.78
13 Feb 2015	139	97	309	2.94
19 Feb 2015	147	n/a	n/a	n/a
03 Mar 2015	193	148	269	3.90

The Cryosphere Discuss., doi:10.5194/tc-2016-84, 2016
Manuscript under review for journal The Cryosphere
Published: 18 April 2016

Figures

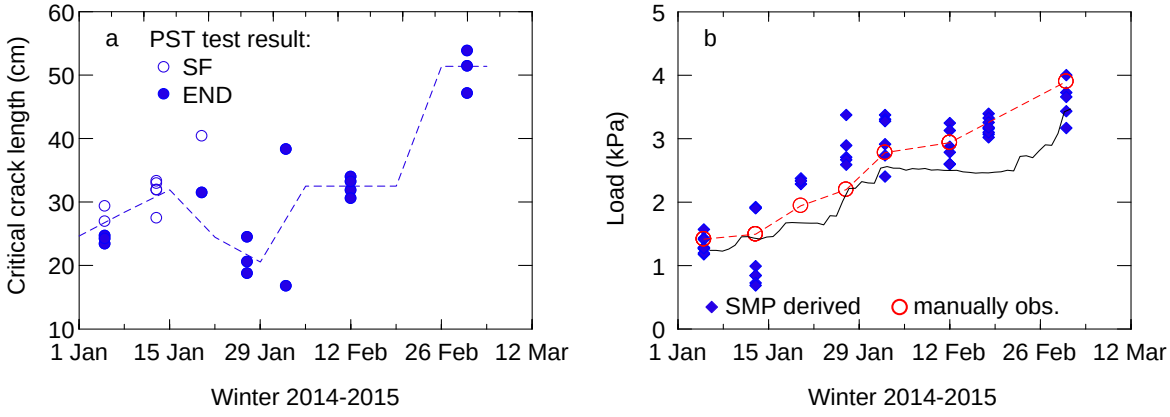

Figure 1: (a) Critical cut length as observed in propagation saw tests (N = 23). Full circles indicate crack propagation to the very end of the column (END), open circles indicate partial propagation resulting in a fracture across the slab (SF); dashed line is a running median smoother. (b) Load on the weak layer: red open circles (connected by dashed line) show the load as calculated from the manually observed density and layer thickness; blue diamonds are corresponding SMP-derived values (N = 50). The black solid line indicates the load as provided by SNOWPACK.

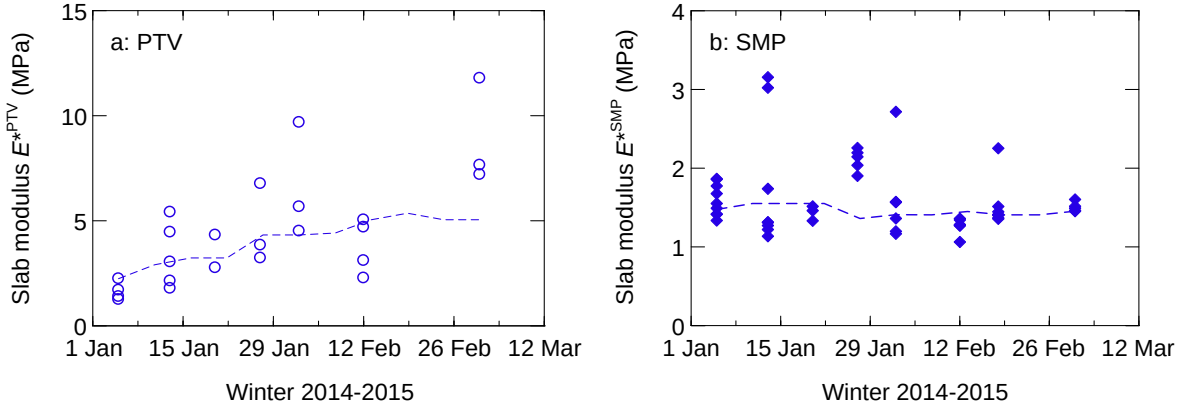

Figure 2: Effective bulk modulus of the slab derived from (a) the bending of the slab via PTV analysis (N = 24), and (b) from the SMP signal analysis (N = 50). Dashed lines are running median smoothers.

The Cryosphere Discuss., doi:10.5194/tc-2016-84, 2016
Manuscript under review for journal The Cryosphere
Published: 18 April 2016

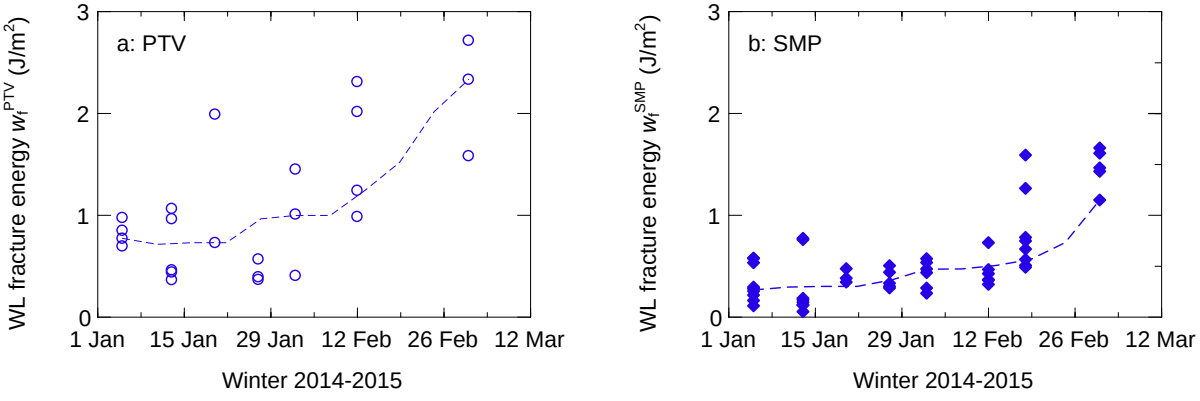

Figure 3: Weak layer fracture energy derived from (a) the bending of the slab via PTV analysis (N = 24), and (b) from the SMP signal analysis (N = 50). Dashed lines are running median smoothers.

The Cryosphere Discuss., doi:10.5194/tc-2016-84, 2016
Manuscript under review for journal The Cryosphere
Published: 18 April 2016

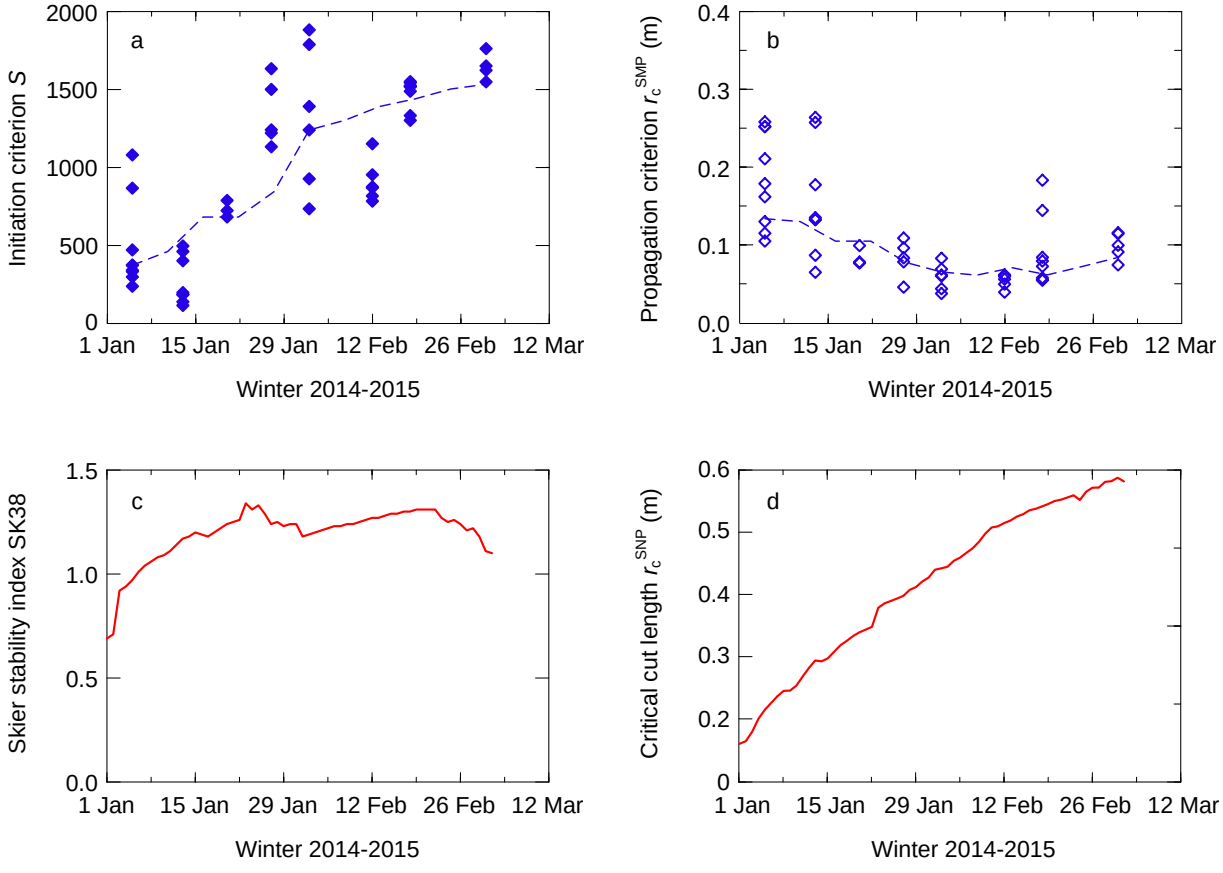

Figure 4: Criterions of instability: (a) SMP-derived failure initiation criterion *S*, and (b) SMP-derived crack propagation criterion r_c^{SMP}; dashed lines are running median smoothers ($N = 50$). Output of the numerical snow cover model SNOWPACK: (c) Skier stability index SK38, and (d) modelled critical cut length r_c^{SNP}.

The Cryosphere Discuss., doi:10.5194/tc-2016-84, 2016
Manuscript under review for journal The Cryosphere
Published: 18 April 2016

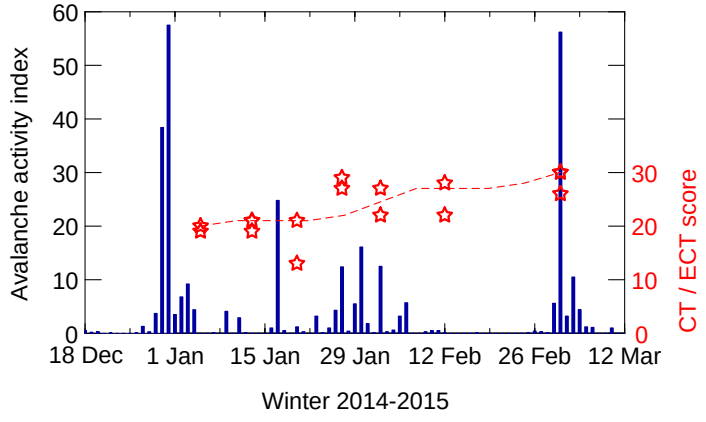

Figure 5: Avalanche activity index for the region of Davos (columns) and results of the CTs and ECTs performed concurrently with the snow profile observations on seven out of eight sampling days (asterisks), the number of taps (score) is shown.

The Cryosphere Discuss., doi:10.5194/tc-2016-84, 2016
Manuscript under review for journal The Cryosphere
Published: 18 April 2016

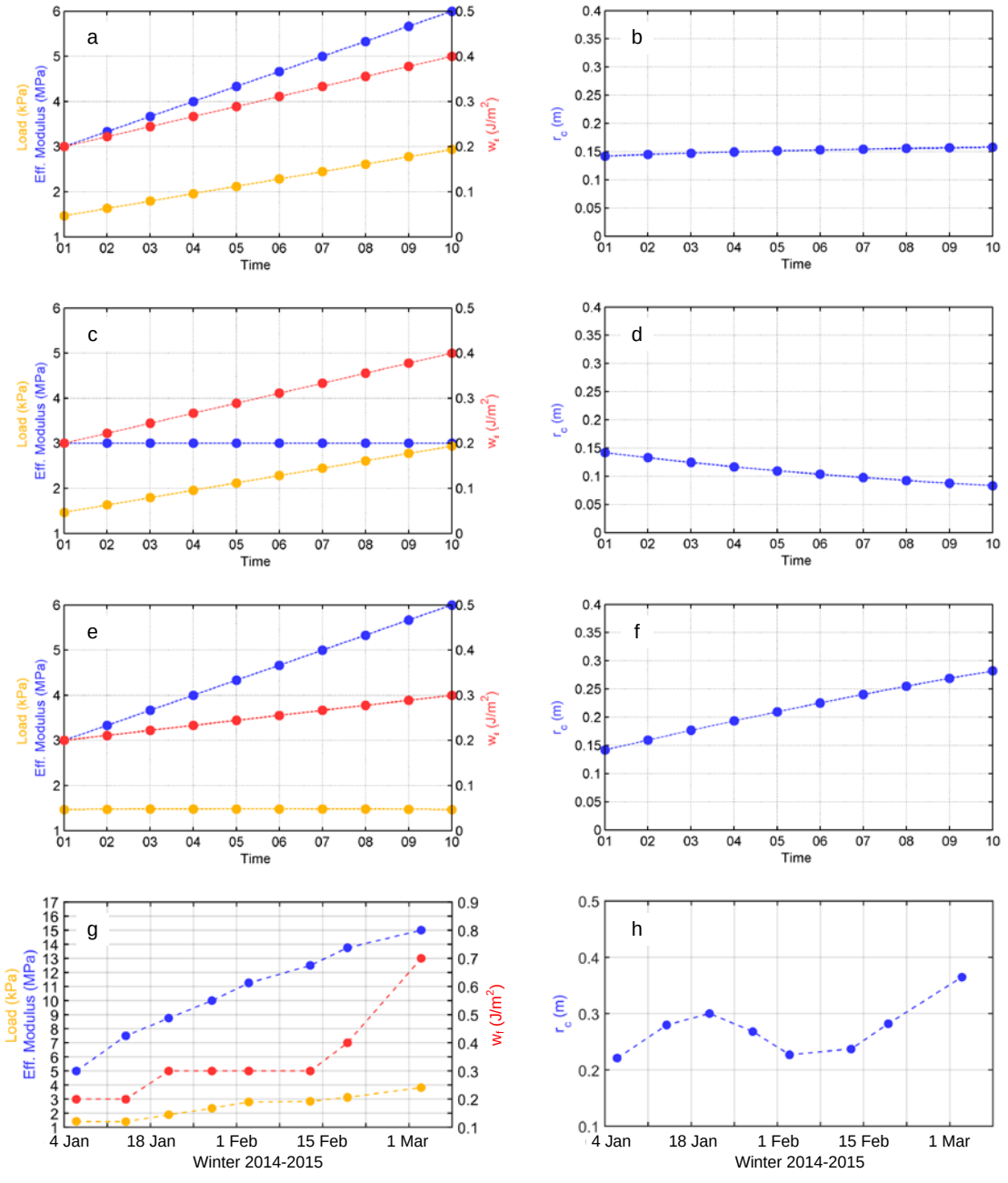

Figure 6: Sensitivity study on how the critical cut length r_c varies as a function of the load and the effective modulus of the slab, and the specific fracture energy of the weak layer w_f. Arbitrary units of time for the three simplified scenarios shown in panels (a) to (f). In the last scenario (g,h), the situation during the sampling period is supposed to be roughly mimicked.